Optics Communications 281 (2008) 5768–5770

Contents lists available at ScienceDirect

Optics Communications

journal homepage: www.elsevier.com/locate/optcom

Wavelength-encoded fiber-optic temperature sensor with ultra-high sensitivity

Enbang Li *, Gang-Ding Peng

College of Precision Instrument and Optoelectronics Engineering, Tianjin University, Tianjin 300072, PR China
School of Electrical Engineering and Telecommunications, University of New South Wales, Sydney, NSW 2052, Australia

ARTICLE INFO

Article history:
Received 26 May 2008
Received in revised form 15 August 2008
Accepted 15 August 2008

Keywords:
Optical fibers
Fiber-optic sensors
Thermo-optic materials
Modal interference
Temperature

ABSTRACT

We present in this paper a wavelength-encoded fiber-optic temperature sensor with ultra-high sensitivity. The sensor consists of a segment of multimode fiber (MMF) with a polymer cladding spliced between two single mode fibers, forming a multimode fiber interferometer. For a temperature sensor with a 55 mm long MMF and a 45 mm long polymer cladding, a temperature sensitivity of −3.195 nm/°C has been achieved over a temperature range of 10 °C which is mainly limited by the spectral range of the light source used in the experiments. It has been found that the high temperature sensitivity is mainly attributed to the high thermo-optic coefficient of the polymer cladding. Other advantages of the temperature sensor reported here include its extremely simple structure and fabrication process, and hence a very low cost.

1. Introduction

Fiber-optic temperature sensors could be the first fiber sensors realized by employing optical fiber technologies and nowadays are still experiencing rapid developments. This is because that fiber-optic temperature sensors offer unique advantages, such as immunity to electromagnetic interferences, good stability and repeatability, superior durability against harsh environments, high sensitivity, high resolution, and fast response. Although various sensing schemes have been proposed and developed, they can be classified into two main categories: intensity-based and wavelength-encoded. The wavelength-encoded temperature sensing methods are more attractive for remote sensing and multipoint applications since the wavelength-encoded temperature information will not change as the optical signal attenuates along the transmission line, and the wavelength multiplexing scheme can be adopted. So far wavelength-encoded temperature sensing has been achieved by using different methods including fiber Bragg gratings (FBGs), long-period fiber gratings (LPGs), fiber Fabry-Perot (FP) cavities, microstructured optical fiber (MOF) tapers, and multimode interference (MMI) based fiber structures [1–10]. It has been demonstrated that LPGs when used in air can have a temperature sensitivity in the range of −140 to −340 pm/°C which is much higher than those of other temperature sensors mentioned above (normally in a range of 11–15 pm/°C).

The temperature sensitivity is an important parameter since it determines the resolution and accuracy of the sensing system and also the wavelength demodulation schemes to be used. A temperature sensor with a high sensitivity allows a low-cost wavelength demodulator to be utilized while still maintaining the required performance.

In this paper, we present a wavelength-encoded fiber-optic temperature sensor with a high sensitivity by utilizing multimode interference (MMI) of higher-order modes in a circular multimode fiber (MMF) with a polymer material as the fiber cladding. The proposed temperature sensor consists of a lead-in single-mode fiber (SMF), a lead-out SMF, and a segment of MMF spliced between the SMFs. The polymer cladding has a large negative thermo-optic coefficient (TOC), which contributes to the enhancement of the temperature sensitivity. In order to further enhance the temperature sensitivity, a packaging material with a large coefficient of thermal expansion (CTE) has been used.

2. Sensing principle and analysis

With optical fibers, MMI can be realized by using a single mode–multimode–single mode (SMS) structure, as described in Ref. [11]. It has been demonstrated that a SMS structure with an optimized length for a given multimode fiber can generate interference maxima or minima in the transmission spectrum, and can be used for strain and temperature sensing [8,12] as well as optical filtering [13]. The relative wavelength shift caused by temperature variations can be expressed as [8]

* Corresponding author. Address: College of Precision Instrument and Optoelectronics Engineering, Tianjin University, Tianjin 300072, PR China. Tel.: +86 2227403206.
E-mail address: enbang@tju.edu.cn (E. Li).

0030-4018/$ - see front matter © 2008 Elsevier B.V. All rights reserved.
doi:10.1016/j.optcom.2008.08.022

$$\frac{\Delta\lambda_1}{\lambda} = (\alpha_1 + \xi_1)\Delta T, \tag{1}$$

where α_1 and ξ_1 are, respectively, the CTE and TOC of the MMF core material. It can be seen that an increase in temperature will cause the transmission spectrum moving linearly to longer (red-shifted) wavelengths and the slop of the temperature dependence is completely determined by the characteristics of the MMF core material.

The wavelength shift introduced by an axial strain applied to the SMS structure is [12]

$$\frac{\Delta\lambda_2}{\lambda} = -(1 + 2v + P_e)\varepsilon, \tag{2}$$

where v is Poisson's ratio of the MMF core, and P_e is the effective strain-optic coefficient of the MMF core material. It is obvious that an axial tensile strain will cause a blue-shift to the transmission spectrum of the SMS device.

The SMS fiber structure is also sensitive to the changes of the refractive index of the polymer cladding. Suppose that the TOC of the polymer cladding is ξ_2, the wavelength shift caused by the refractive index variations induced by temperature changes can be expressed as

$$\frac{\Delta\lambda_3}{\lambda} = \chi\xi_2\Delta T, \tag{3}$$

where χ is a constant. When ξ_2 is negative, the thermo-optic effect of the polymer cladding introduces a negative temperature sensitivity to the sensor.

The combined wavelength shift caused by the temperature variation and strain would be

$$\begin{aligned}\Delta\lambda &= \Delta\lambda_1 + \Delta\lambda_2 + \Delta\lambda_3 \\ &= \lambda[(\alpha_1 + \xi_1)\Delta T - (1 + 2v + P_e)\varepsilon + \chi\xi_2\Delta T].\end{aligned} \tag{4}$$

Suppose that the single mode fibers and the MMF core have an identical diameter and an identical CTE. When we bond the ends of the SMS structure to a packaging material with a CTE, α_2, as shown in Fig. 1, the axial strain caused by the difference in CTEs would be

$$\varepsilon = (\alpha_2 - \alpha_1)\Delta T. \tag{5}$$

Substituting Eq. (5) into Eq. (4), one obtains

$$\Delta\lambda = \lambda[(\alpha_1 + \xi_1 + \chi\xi_2) - (1 + 2v + P_e)(\alpha_2 - \alpha_1)]\Delta T. \tag{6}$$

It can be seen from Eq. (6) that the wavelength shift is proportional to the temperature variation, and the temperature sensitivity is determined by the thermal properties of the MMF core material, the packaging material and the polymer cladding. For silica fibers, $\alpha_1 = 5 \times 10^{-7}$; $\xi_1 = 6.9 \times 10^{-6}/°C$; $p_e = 0.22$, and $v = 0.16$. If a packaging material with a large CTE and a polymer cladding with a large negative TOC are used for fabricating the temperature sensor, then the sensor will have a negative and enhanced temperature sensitivity.

3. Sensor fabrication and tests

In order to experimentally demonstrate the proposed temperature sensing method, we fabricated SMS temperature sensors by using the standard communications fibers (Corning SMF 28) as the lead-in and lead-out fibers. The MMF (provided by Nufern) used in the experiments had a silica core with a diameter of 125 μm, and a polymer cladding with a diameter of 250 μm. The length of the MMF segment was 55 mm and the length of the polymer cladding was 45 mm. A fusion splicer (Fitel S175) was used to fabricate the devices. The packaging material employed in our experiments was an aluminum tube with a CTE of $\alpha_2 = 22 \times 10^{-6}/°C$. As shown in Fig. 1, the SMF ends of the SMS structure were bonded to the aluminum tube by using epoxy.

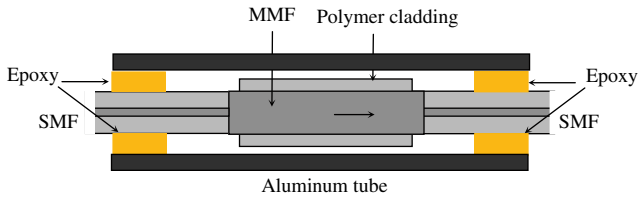

Fig. 1. Schematic diagram of the developed temperature sensor.

To measure the transmission spectra of the temperature sensor, the lead-in fiber of the sensor was connected to an ASE broadband source with an output power of 5 mW and a central wavelength of 1550 nm and a bandwidth of about 35 nm. An optical spectrum analyzer (OSA, YOKOGAWA AQ6317C) was used to record the transmission spectra and to measure the wavelength shifts. The OSA has a wavelength resolution of 10 pm. By using the curve fitting and bottom searching functions provided with the OSA, a resolution of 1 pm could be achieved. Fig. 2 shows two transmission spectra of the fabricated temperature sensor recorded at 32.5 °C and 34.5 °C, respectively. From the measured transmission spectra, a number of features can be noted. It can be seen that the modal interferences in the MMF segment produce fluctuations in the transmission spectra. As shown in Fig. 2a, in the spectrum recorded at 32.5 °C a large dip appears besides a few of smaller peaks and troughs. At different temperatures, the shape of the transmission spectrum will vary. This is because that the inherent thermal expansion, photoelastic and thermo-optic effects of the fiber materials not only affect the propagation constants of the fiber modes

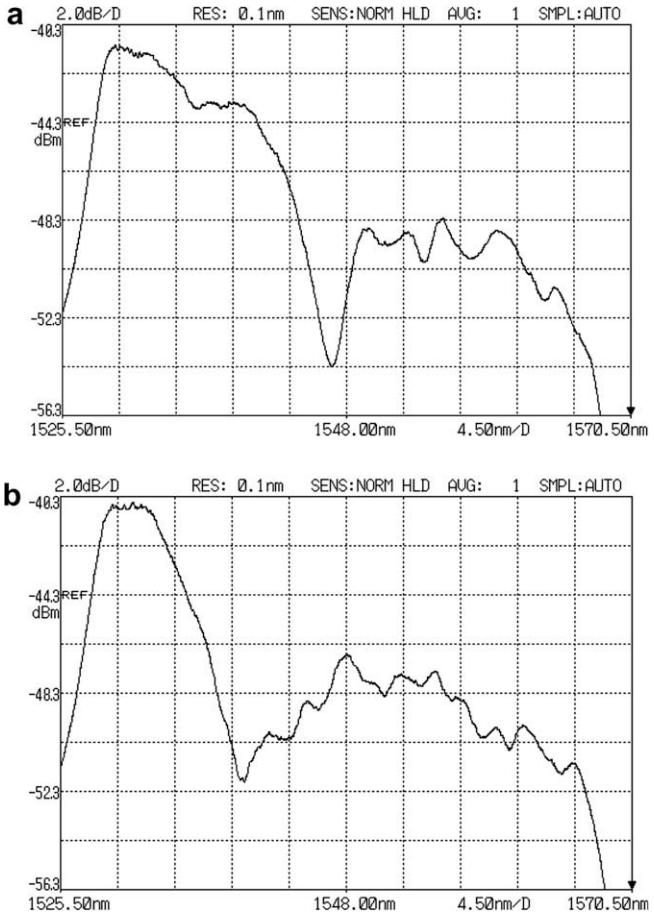

Fig. 2. Measured transmission spectra of the temperature sensor at 32.5 °C (a) and 34.5 °C (b), respectively.

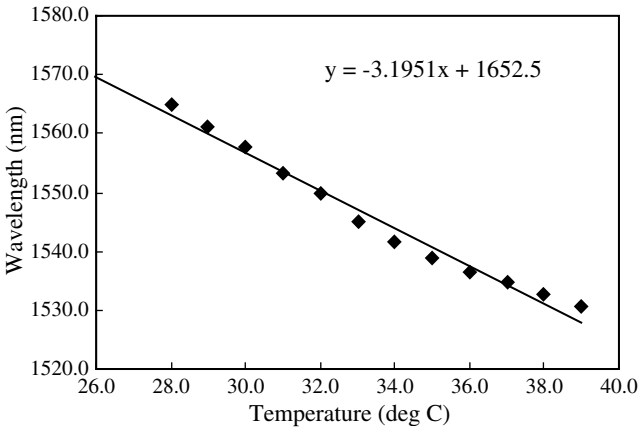

Fig. 3. Measured wavelength shifts at different temperatures.

involved in the modal interferences, but also cause variations of the modal energy distribution among these modes. Fig. 2b shows a spectrum recorded at 34.5 °C, which is quite different from the one measured at 32.5 °C. In principle, each of these peaks and troughs can be utilized as wavelength markers for temperature sensing purposes. In practice, the most prominent interfering minimum or maximum is normally used as a wavelength marker. We note that the largest dip in the spectrum shifted to a shorter wavelength when the temperature was changed from 32.5 °C to 34.5 °C.

In order to characterize the fabricated temperature sensor, a temperature measurement experiment was carried out. The temperature sensor was positioned in an environmental chamber (Espec SH641) to control the temperature with an accuracy of 0.1 °C. Before the temperature measurement tests, the fabricated sensor was temperature-cycled between −10 °C and 60 °C for strain relaxation.

Plotted in Fig. 3 are the wavelength shifts measured at different temperatures from 28 °C to 39 °C. It can be seen that the wavelength shift decreases when the temperature is increased, and a nearly linear relation exists. A linear curve fit to the experimental data reveals an average slop of −3.195 nm/°C. The temperature range which could be measured by the sensor was limited by the spectral range (35 nm) of the light source available in the experiment.

From Eqs. (1), (2), and (5), and using the fiber parameters and the packaging material properties, we calculated the temperature sensitivity (without taking the thermo-optic effect of the polymer cladding into account) at the 1550 nm band as −39.85 pm/°C, which is much lower than the overall temperature sensitivity of the developed sensor. In order to identify the contribution of the aluminum packaging material to the temperature sensitivity, we also carried out a separate test with an unpackaged sensor which had identical structure and fiber parameters with the packaged sensor (but without the aluminum tube). The results show that the unpackaged sensor has a temperature sensitivity of −2.72 nm/°C, which is 0.475 nm/°C lower than that of the packaged sensor. Using Eqs. (2) and (5), we calculated the contribution of the aluminum packaging material to the temperature sensitivity of the packaged sensor as 0.513 nm/°C. We can therefore conclude that the thermo-optic effect of the polymer cladding makes a significant contribution to the sensitivity of the packaged temperature sensor. The exact figure of the TOC of the polymer coating, ξ_2, is not specified, but is known to be in the -10^{-4}/°C range, which is two order of magnitude larger than other thermal parameters of silica materials.

It should be noted that the measurement range of the temperature sensor is mainly determined by the spectral range of the light source as the interference dip used for the temperature measurement could move out of the spectral range. With the current experimental set-up, a 35 nm spectral range allows a measurement range of about 10 °C. One method for extending the measurement range is to switch to another interference dip which is within the available spectral range.

We also noted that the shapes of the transmission spectrum of the fabricated temperature sensors vary from one to another, which may be caused by slight differences in the splicing processes involved in the fabrication of individual sensors. However, temperature measurements will not be affected once a prominent interfering minimum or maximum can be identified, which is the main advantage of a wavelength-encoded fiber-optic temperature sensor.

4. Conclusion

In conclusion, we have proposed and demonstrated a wavelength-encoded fiber-optic temperature sensor with an ultra-high sensitivity. The sensor consists of a segment of MMF with a polymer cladding spliced between two single-mode fibers, forming a multimode interferometer. For a sensor with a 55 mm long MMF and a 45 mm long polymer cladding, a temperature sensitivity of −3.195 nm/°C has been achieved over a temperature range of 10 °C. The demonstrated temperature sensitivity is much higher than those of the FBG and LPG based temperature sensors previously reported. The measurement range is limited by the spectral range of the light source. It has been found that the high temperature sensitivity is mainly attributed to the high TOC of the polymer coating. Compared to other fiber-optic temperature sensors, the sensors reported here feature an extremely simple structure and fabrication process, and hence a very low cost.

Acknowledgements

This work was supported by Natural Science Foundation of China (Grant No. 60578054) and Tianjin Municipal Science and Technology Commission (Grant No. 08JCZDJC19300).

References

[1] R.M. Measures, Structural Monitoring with Fiber Optic Technology, Academic, San Diego, CA, 2001.
[2] A. Othonos, K. Kalli, Fiber Bragg Gratings: Fundamentals and Applications in Telecommunications and Sensing, Artech House, Boston, MA, 1999.
[3] K.O. Hill, G. Meltz, J. Lightwave Technol. 15 (1997) 1263.
[4] A.D. Kersey, M.A. Davis, H.J. Patrick, M. LeBlanc, K.P. Koo, C.G. Askins, M.A. Putnam, E.J. Friebele, J. Lightwave Technol. 15 (1997) 1442.
[5] X. Shu, L. Zhang, I. Bennion, J. Lightwave Technol. 20 (2002) 255.
[6] X. Chen, F. Shen, Z. Wang, Z. Huang, A. Wang, Appl. Opt. 45 (2006) 7760.
[7] D. Monzón-Hernández, V.P. Minkovich, J. Villatoro, IEEE Photon. Technol. Lett. 18 (2006) 511.
[8] E.B. Li, X.L. Wang, C. Zhang, Appl. Phys. Lett. 89 (2006) 91119.
[9] J. Jung, H. Nam, B. Lee, J.O. Byun, N.S. Kim, Appl. Opt. 38 (1999) 2752.
[10] Y. Zhan, H. Cai, G. Kan, R. Qu, S. Xiang, Z. Fang, Proc. SPIE. 5279 (2004) 661.
[11] D. Donlagic, B. Culshaw, J. Lightwave Technol. 17 (1999) 1856.
[12] E.B. Li, IEEE Photon. Technol. Lett. 19 (2007) 1266.
[13] W.S. Mohammed, P.W.E. Smith, X. Gu, Opt. Lett. 17 (2006) 2547.